

Superconducting Transition in YBCO Bulk Ceramics: Correlating Sintering Temperature, Phase Formation, and AC Susceptibility

(Peralihan Superkonduktor dalam Seramik Pukal YBCO: Menghubungkan Suhu Pensinteran, Pembentukan Fasa dan Kecenderungan AC)

RYAD ALHADEI MOHAMED AREBAT^{1,2}, MOHD MUSTAFA AWANG KECHIK^{1,*}, CHEN SOO KIEN¹, LIM KEAN PAH¹, HOO KEONG PEH¹ & ABDUL HALIM SHAARI¹

¹*Superconductor & Thin Films Laboratory, Department of Physics, Faculty of Science, Universiti Putra Malaysia, 43400 UPM Serdang, Selangor, Malaysia*

²*Department of Physics, Faculty of Science, El-Mergib University, Al Khums City, Libya*

Received: 10 October 2024/Accepted: 16 December 2024

ABSTRACT

Sintering significantly influences the phase composition and crystal structure of high-temperature superconductors, such as yttrium barium copper oxide ($\text{YBa}_2\text{Cu}_3\text{O}_{7-\delta}$, YBCO) bulk ceramics, thereby impacting their superconductivity. This study investigates the effects of various sintering temperatures (920 °C, 950 °C, and 980 °C) on phase formation, AC susceptibility, and the superconducting transition temperature (T_c) in pure YBCO bulk ceramics synthesized via traditional solid-state reaction method (SSR). Characterization techniques employed include X-ray diffraction (XRD), AC susceptibility (ACS), and temperature-dependent resistance measurements via the four-point probe method (4PP). XRD analysis confirmed the predominance of the YBCO phase across all samples, with the highest phase purity (98.9%) and optimal oxygen content achieved at 980 °C. The superconducting transition temperature $T_{c\text{-onset}}$ measured by ACS for the sample sintered at 980 °C was 93.21 K, while 4PP yielded a $T_{c\text{-onset}}$ of 91.28 K; both values decreased at lower sintering temperatures. Notably, the superconducting transition width (ΔT_c) narrowed with increasing sintering temperature, with the sharpest transition observed at 980 °C, indicating enhanced phase homogeneity and intergranular connectivity. Additionally, the critical current density (J_{cm}) at the peak temperature (T_p) of the imaginary part (χ'') was calculated using the Bean critical state model, revealing a maximum J_{cm} of 7.639 A/cm² for the sample sintered at 980 °C.

Keywords: AC susceptibility (ACS); sintering temperature; superconducting transition temperature (T_c); X-ray diffraction (XRD); YBCO bulk ceramic

ABSTRAK

Pensinteran memberi pengaruh yang ketara terhadap komposisi fasa dan struktur kristal bagi pengalir super suhu tinggi, seperti seramik pukal oksida kuprum barium itrium ($\text{YBa}_2\text{Cu}_3\text{O}_{7-\delta}$, YBCO) yang seterusnya mempengaruhi kekonduksian super mereka. Penyelidikan ini mengkaji kesan pelbagai suhu pensinteran (920 °C, 950 °C dan 980 °C) terhadap pembentukan fasa, kepekaan AC dan suhu peralihan kekonduksian super (T_c) dalam seramik pukal YBCO tulen yang disintesis melalui kaedah tindak balas pepejal (SSR). Teknik pencirian yang digunakan termasuk pembelauan sinar-X (XRD), kepekaan AC (ACS) dan pengukuran rintangan bergantung suhu melalui kaedah penduga empat titik (4PP). Analisis XRD mengesahkan dominasi fasa YBCO dalam semua sampel dengan ketulenan fasa tertinggi (98.9%) dan kandungan oksigen yang optimal dicapai pada suhu 980 °C. Suhu peralihan kekonduksian super $T_{c\text{-onset}}$ yang diukur oleh ACS untuk sampel yang disinter pada 980 °C adalah 93.21 K, manakala 4PP menunjukkan $T_{c\text{-onset}}$ sebanyak 91.28 K; kedua-dua nilai tersebut menurun pada suhu pensinteran yang lebih rendah. Secara ketara, lebar peralihan kekonduksian super (ΔT_c) menyempit dengan peningkatan suhu pensinteran, dengan peralihan yang paling tajam diperhatikan pada 980 °C, menunjukkan peningkatan homogeniti fasa dan hubungan antara butir. Tambahan pula, ketumpatan arus kritikal (J_{cm}) pada suhu puncak (T_p) bahagian imajiner (χ'') telah dikira menggunakan model keadaan kritikal Bean, mendedahkan J_{cm} maksimum sebanyak 7.639 A/cm² untuk sampel yang disinter pada 980 °C.

Kata kunci: Kepekaan AC (ACS); pendifraksian sinar-X (XRD); seramik pukal YBCO; suhu pensinteran; suhu peralihan kekonduksian super (T_c)

INTRODUCTION

High-temperature superconductors (HTS) such as $\text{YBa}_2\text{Cu}_3\text{O}_{7-\delta}$ (YBCO) are pivotal in various industries, including energy, transportation, electronics, and healthcare, due to their zero-resistance properties at elevated temperatures. Considerable efforts have been dedicated to synthesizing YBCO bulk ceramic through a variety of methods, including wet and dry chemical techniques such as thermal treatment (TT) (Mustafa Mousa et al. 2017; Nur Athirah et al. 2022), modified thermal decomposition (DM) (Nur Afifah et al. 2024; Ryad Alhadei et al. 2024b), sol-gel (Aşıkuzun & Öztürk 2020; Bahboh et al. 2019), and co-precipitation (Nazarudin et al. 2011; Nurhidayah et al. 2017). Despite advancements in these techniques, the solid-state reaction (SSR) method remains the most commonly employed approach for YBCO synthesis due to its simplicity, cost-effectiveness, and scalability. Compared to alternative techniques, SSR requires minimal equipment and readily available materials, making it ideal for large-scale production of YBCO (Chin et al. 1987; Ozturk et al. 2019; Ryad Alhadei et al. 2024a).

Heat treatments - such as annealing, calcination, and sintering - are crucial for optimizing the superconducting properties of YBCO bulk ceramics. These processes directly influence phase composition, crystal structure, and sample densification, which in turn affect the critical temperature (T_c) and overall superconducting performance (Hannachi et al. 2022). Sintering, a key heat treatment conducted below the material's melting point, facilitates particle bonding, improves intergranular connectivity, and strengthens grain boundaries, all essential for achieving optimal superconducting characteristics. Typically performed in air or oxygen flow, sintering promotes phase stabilization, enhancing material strength and structural integrity. Conducting sintering in ambient conditions can further simplify the process, reducing costs and processing time without compromising material performance (Hannachi et al. 2022; Nurhidayah et al. 2017; Pruss et al. 1989). While prior research has explored the influence of sintering temperature on the properties of YBCO, a comprehensive understanding of the specific correlations between sintering temperature, phase purity, AC susceptibility, and four-point probe measurements remains limited. This study systematically varies sintering temperatures and conducts thorough characterization to investigate the relationships among sintering temperature, phase formation, and AC susceptibility response in YBCO ceramics.

In this investigation, YBCO bulk were synthesized using the SSR method and subjected to three distinct sintering temperatures: 920 °C, 950 °C, and 980 °C. The selection of these temperatures is informed by previous studies indicating that sintering near the YBCO melting point enhances phase formation and superconducting properties (Mohammad & Mohammad Reza 2020; Mustafa Mousa et al. 2017). Additionally, our choice of temperatures was validated using a thermogravimetric analyzer (TGA)

(Yap et al. 2024c). This temperature selection strategy, based on existing research, suggests that sintering in proximity to the YBCO melting point yields superior phase formation and superconducting characteristics (Abdul Hussein, Hussein & Hasan 2023; Jin et al. 2017). By linking these factors to the superconducting transition temperature (T_c), this study aims to provide clear insights into improving the performance of YBCO superconductors.

EXPERIMENTAL DETAILS

Superconducting YBCO bulk ceramics were synthesized using SSR. High-purity Y_2O_3 , BaCO_3 , and CuO powders (99.99%) were combined in the stoichiometric ratio Y:Ba: Cu = 1:2:3. The powders were thoroughly mixed and ground for 2 h to ensure homogeneity of the starting materials. The resulting mixture was then calcined at 840 °C for 24 h to facilitate the formation of intermediate phases, leading to the YBCO phase. After calcination, the black solid was further ground for 1 h to improve packing density before being pressed into circular pellets (8 mm diameter, 8 mm thickness). These pellets were subsequently sintered at three different temperatures – 920 °C, 950 °C, and 980 °C - for 24 h each, allowing sufficient time for grain growth and phase transformation. Following sintering, the pellets were slowly cooled and then subjected to final annealing at 600 °C for 12 h in an ambient atmosphere to optimize the crystal structure.

A Mettler Toledo thermogravimetric analyzer (model TGA/SDTA851e, Mettler Toledo, Zürich, Switzerland) was employed to investigate the thermal characteristics of YBCO powders. The samples were subjected to heating up to 1000 °C at a 10 °C/min rate in a nitrogen environment, with a gas flow of 50 mL/min. X-ray diffraction (XRD) was conducted to study phase development and crystal structure in the specimens, utilizing a Philips Xpert Pro Analytical diffractometer (model DY 1861, Philips, Eindhoven, The Netherlands) with $\text{CuK}\alpha$ radiation, scanning from $2\theta = 20^\circ$ to 80° . The four-point probe method was used to evaluate electrical transport properties, employing a digital nanovoltmeter (Keithley, Model 2182A, Cleveland, OH, USA) and DC precision power source (Keithley, Model 6221, Cleveland, OH, USA). To determine the superconducting transition temperature (T_c), magnetic properties were assessed through AC susceptibility (ACS) measurements, using an SR830 lock-in amplifier at 219 Hz frequency with a 1.0 Oe applied magnetic field. Bulk samples measuring (4.5 mm × 2.0 mm × 1.50 mm) were prepared for these measurements.

RESULTS AND DISCUSSION

THERMOGRAVIMETRIC ANALYSIS (TGA) AND DIFFERENTIAL THERMOGRAVIMETRICS (DTG)

The TGA and DTG curves for the YBCO bulk ceramic provide detailed insights into its thermal stability and

decomposition behavior, which are critical for determining optimal calcination and sintering temperatures (Figure 1). The analysis identifies four distinct weight-loss stages, each corresponding to specific thermal events. The first stage, occurring at approximately 57 °C, shows a weight loss of 5.71%, which is attributed to the evaporation of moisture and adsorbed water. Moreover, the DTG curve displays a gradual decline during this phase, which aligns with previous reports on the dehydration process in YBCO materials (Kamarudin et al. 2022; Yap et al. 2024c). The second stage, observed between 230.06 °C and 346.51 °C, is marked by a 2.32% weight loss. This phase is associated with the decomposition of organic residues and the evolution of gases, including CO₂, as indicated by an exothermic peak in the DTG curve. Furthermore, this step is crucial for removing residual impurities, as their presence could hinder the purity of the final Y-123 phase and negatively affect its superconducting properties (Aima 2018). The third stage, spanning 733 °C to 893.54 °C, results in a 6.54% weight loss and is characterized by the breakdown of remaining volatile components and barium-based compounds. Consequently, the DTG curve displays a prominent exothermic peak, signifying a pivotal phase in the formation of the stable YBCO crystal structure. Previous studies have emphasized the importance of this temperature range in facilitating phase formation (Dubinsky et al. 2005; Hong et al. 2023). Finally, at temperatures exceeding 893.54 °C, the transformation of precursor materials into their respective metal oxides takes place. Notably, the DTG curve exhibits a thermal event at approximately 873 °C, indicating the onset of Y-123 phase formation. This stage is critical for the development of the orthorhombic structure, which defines YBCO's superconducting properties. Furthermore, the orthorhombic

structure stabilizes fully by around 920 °C, consistent with findings from prior research (Jin et al. 2017; Ryad Alhadei et al. 2024a; Yap et al. 2024c). Thermal analysis shows that the optimal calcination temperature for YBCO lies within 840 °C to 950 °C, ensuring intermediate phase formation and the elimination of volatiles. Additionally, sintering at temperatures between 950 °C and 980 °C is necessary to stabilize the orthorhombic Y-123 phase and achieve superior superconducting properties (Pathak et al. 2001; Yap et al. 2024c; Yeoh & Abd-Shukor 2008).

X-RAY DIFFRACTION ANALYSIS

The X-ray diffraction (XRD) patterns for YBCO samples sintered at 920 °C, 950 °C, and 980 °C are shown in Figure 2, analyzed within a 2θ range of 20°-80°. The data were processed using X'Pert Highscore Plus software, which incorporates Rietveld refinement and the Inorganic Crystal Structure Database (ICSD) (Nur Afiqah et al. 2024). The analysis confirms that the dominant Y-123 orthorhombic phase was observed in all samples, with no evidence of an orthorhombic-tetragonal phase transition (ICSD: 98-003-1706). A minor secondary phase of Y₂BaCuO₅ (Y-211) (ICSD: 98-002-4901) and CuO (ICSD: 98-008-7542) was detected. The impurity peaks located at 30.50°, 29.82°, 31.60°, 35.45°, and 38.73° were more pronounced in the sample sintered at 920 °C compared to those sintered at higher temperatures. Specifically, the sample sintered at 950 °C exhibited a phase purity of 98.4%, while the sample sintered at 980 °C exhibited a purity of 98.9%. This suggests that sintering at 950 °C and 980 °C is more conducive to achieving a higher purity Y-123 phase (Hannachi et al. 2022). Furthermore, the weight fraction of the YBCO phase was higher in the

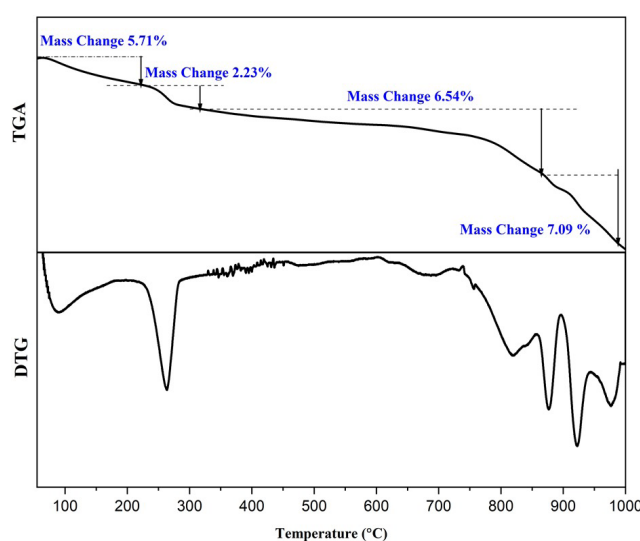


FIGURE 1. Thermogravimetric (TGA) and derivative thermogravimetric (DTG) curves of uncalcined YBa₂Cu₃O_{7-δ} (YBCO) bulk ceramic

samples sintered at 950 °C and 980 °C compared to the sample sintered at 920 °C (Pruss et al. 1989) (Table 1). In all samples, the most intense diffraction peak, observed at approximately $2\theta \approx 32.89^\circ$, corresponds to the [103] Miller indices of the YBCO-123 phase, confirming the dominant orthorhombic structure. The calculated lattice parameters (a , b , and c), along with the orthorhombicity factor and oxygen content for all samples, are summarized in Table 1. These structural details further corroborate the phase purity and crystal structure stability, with higher sintering temperatures promoting improved phase formation and reduced impurity levels.

Previous studies have demonstrated that even slight variations in oxygen content can significantly influence the crystal structure and superconducting transition temperature (T_c) of YBCO (Benzi, Bottizzo & Rizzi 2004; Chen et al. 2022; Hannachi et al. 2022; Kulpa et al. 1989; Zhou et al. 2013). In this study, samples annealed at different temperatures exhibited noticeable differences in oxygen content. The specimen sintered at 920 °C had a slightly lower oxygen content compared to the one sintered at 980 °C, with an approximate variation of $\Delta\delta \approx 0.0007$. Although this difference in oxygen content may seem minimal, it was sufficient to cause discernible changes in both the crystal structure and T_c , aligning with prior research findings (Cheong & Chen 2024; Nurhidayah et al. 2017). The oxygen content ($7-\delta$) was determined using the formula $7-\delta = 75.250 - 5.856c$, which relates the oxygen deficiency to the c-axis lattice parameter (Benzi, Bottizzo & Rizzi 2004). Variations in the oxygen content can directly affect the orthorhombic distortion and, consequently, the superconducting properties of Y-123 ceramics. As shown in Table 1, the slight differences in the orthorhombicity factor further substantiate the impact of sintering temperature on the oxygen stoichiometry and crystal structure (Campi et al. 2014; Farneth et al. 1988). The primary elements affecting the crystal structure and superconducting characteristics of pure YBCO ceramics are most likely associated with phase composition and orthorhombicity factor (Reissner et al. 1990). Table 2 summarizes the volume fraction, unit cell volume (V), and crystallite size of the samples. As the sintering temperature increased from 920 °C to 980 °C, the crystallite size grew, suggesting a tendency for crystallites to coalesce at higher temperatures. This phenomenon suggests that higher sintering temperatures enhance grain connectivity and phase purity. The increased weight fraction of the Y-123 phase at elevated temperatures, as evidenced by the XRD patterns, also contributes to an improved critical temperature (T_c). This correlation between higher phase purity and elevated T_c has been consistently reported in prior studies (Mustafa Mousa et al. 2017; Nurhidayah et al. 2017; Pathak et al. 2001). The results indicate that optimizing sintering temperature not only augments phase purity but also significantly boosts the superconducting properties, as demonstrated by the elevated T_c in samples sintered at higher temperatures.

ELECTRICAL RESISTIVITY MEASUREMENT

Figure 3(a) presents the resistance-temperature (R vs. T) curves for the Y-123 samples. The normalized resistivity as a function of temperature was measured using the conventional four-point probe (4PP) method, covering a temperature range of 30 to 300 K (Yap et al. 2024b). Figure 3(b) zooms in on the critical temperatures, $T_{c-onset}$ and T_{c-zero} , and width of the resistive transition temperature ΔT_c , which were determined through a derivative analysis of the resistance (dp/dT). This method enhances the precision of critical temperature determination, where $T_{c-onset}$ is defined as the point at which the second derivative of resistance deviates from linearity, and T_{c-zero} is the temperature at which the resistance completely vanished (Yap et al. 2024b, 2024c). As seen in Figure 3(a), all samples exhibit metallic behavior in the normal state, followed by a rapid decline in resistance to zero, signifying a single-step superconducting transition. This indicates good grain connectivity and the predominance of the Y-123 phase, as corroborated by previous studies (Yap et al. 2024a, 2024b). The superconducting properties $T_{c-onset}$, T_{c-zero} and ΔT_c for the samples are provided in Table 3, with the sample sintered at 980 °C showing a higher T_c compared to those sintered at 920 °C and 950 °C (Jin et al. 2017).

The narrower ΔT_c (2.63 K) observed in the 980 °C sample indicates a more homogeneous and well-structured microstructure (Jin et al. 2017). This improvement is attributed to enhanced crystallite size (from 62.8 nm to 142.8 nm), higher orthorhombicity (~ 0.00846), and a more homogeneous distribution of oxygen vacancies (Tables 1 & 2) (Abdul Hussein, Abdul Hussein & Hasan 2023; Mustafa Mousa et al. 2017). These factors contribute to a more interconnected grain structure, facilitating efficient charge carrier transport and resulting in a sharper resistive transition (Howe 2014; Nur Nabilah et al. 2018). The optimized microstructure and phase purity at 980 °C led to improved superconducting properties, including a higher $T_{c-onset}$ and narrower ΔT_c , which are crucial for practical applications of Y-123 superconductors (Abdul Hussein, Abdul Hussein & Hasan 2023; Ryad Alhadei et al. 2024a).

AC SUSCEPTIBILITY ANALYSIS

Figure 4 shows the temperature dependencies of the real (χ') and imaginary (χ'') parts of AC susceptibility (ACS) for YBCO samples sintered at different temperatures 920 °C, 950 °C, and 980 °C. The measurements were taken under an AC magnetic field of 1.0 Oe at a frequency of 219 Hz. The real part (χ') primarily reflects the diamagnetic response of the material, while the imaginary part (χ'') relates to flux pinning strength and the intergranular connectivity of the grains (Barood et al. 2023; Kameli, Salamati & Abdolhosseini 2008). In the real part (χ'), typically two transitions are observed: the first at $T_{c-onset}$, which corresponds to the intragrain superconducting

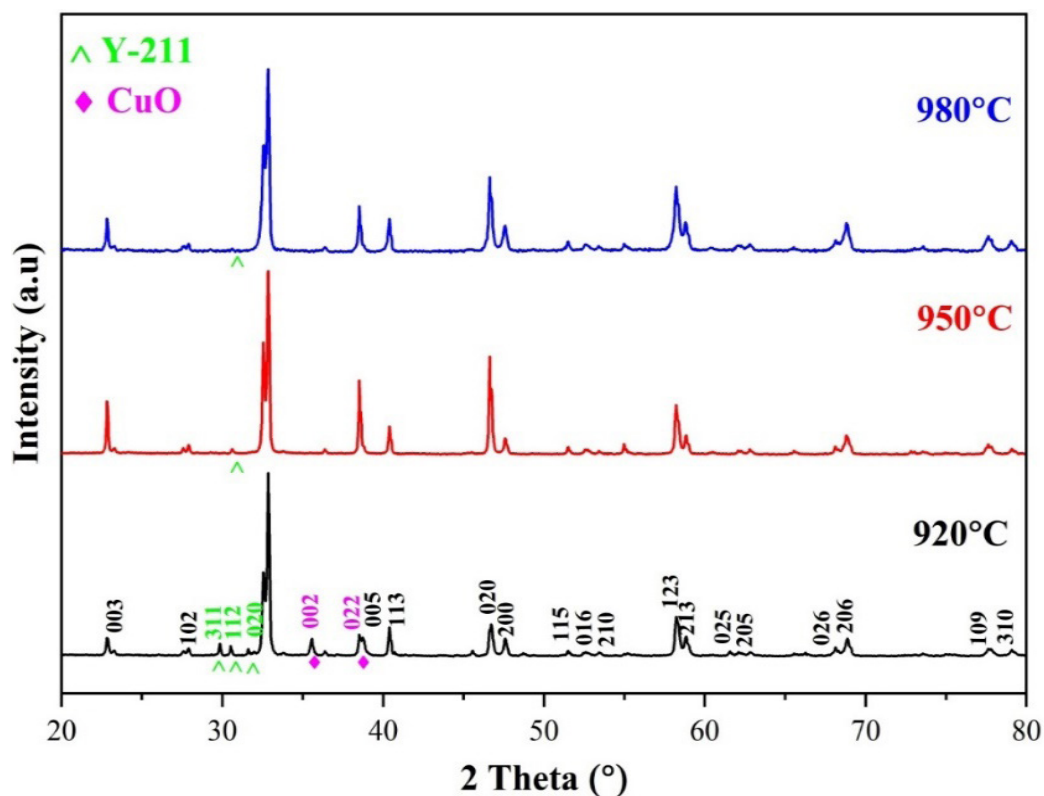


FIGURE 2. X-ray diffraction (XRD) patterns of YBCO samples sintered at 920 °C, 950 °C, and 980 °C

TABLE 1. Lattice parameters, orthorhombicity factor, and oxygen content of YBCO samples at different sintering temperatures

Sintering temperature (°C)	Lattice parameters (Å)			Orthorhombicity factor (Å)	$O_{7-\delta}$
	<i>a</i>	<i>b</i>	<i>c</i>		
920	3.8212	3.8850	11.6811	0.00828	6.8454
950	3.8230	3.8868	11.6827	0.00827	6.8361
980	3.8202	3.8854	11.6810	0.00846	6.8461

TABLE 2. Volume fraction, unit cell volume, and crystallite size of YBCO samples at different sintering temperatures

Sintering temperature (°C)	Volume fraction %			V^3 (Å ³)	Crystalline size (nm)
	$YBa_2Cu_3O_7$	Y_2BaCuO_7	CuO		
920	79.5	7.5	13	173.41	92.0
950	98.4	1.6	/	173.60	62.8
980	98.9	1.1	/	173.38	142.8

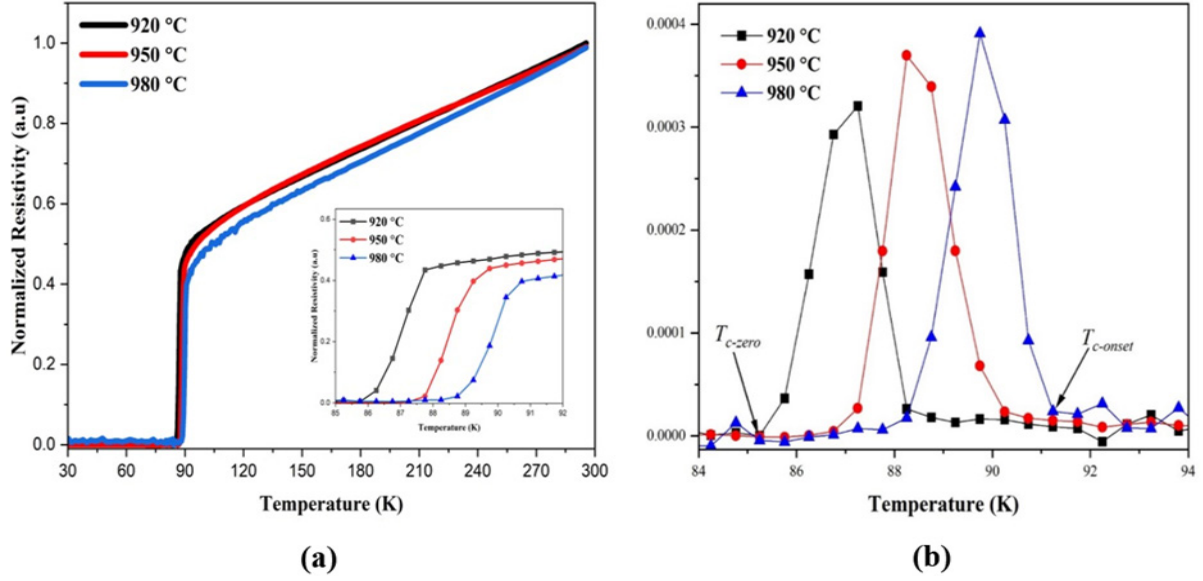


FIGURE 3. (a) Normalized resistance as a function of temperature for YBCO samples sintered at 920 °C, 950 °C, and 980 °C; (b) Temperature derivative of resistivity ($d\rho/dT$) for YBCO samples

TABLE 3. Properties of superconducting transition temperature: $T_{c-onset}$, T_{c-zero} and ΔT_c of the samples

Sintering temperatures (°C)	$T_{c-onset}$ (K)	T_{c-zero} (K)	ΔT_c (K)
920	88.24	85.24	3.00
950	90.25	86.75	3.50
980	91.28	88.65	2.63

transition, and the second, known as the phase lock-in temperature (T_{cl}), indicating intergrain superconducting coupling (Nur-Akasyah, Ranjbar & Abd-Shukor 2021; Nur Nabilah et al. 2018). However, in this study, only a single transition peak corresponding to $T_{c-onset}$ is observed in all samples. The absence of (T_{cl}) could be attributed to a broad superconducting transition, noise in the signal, or ACS sensitivity to phase changes during the transition. This phenomenon has been reported in Y-123 materials where $T_{c-onset}$ is easier to detect than (T_{cl}) (Nur-Akasyah, Abd-Shukor & Chong 2023; Nur-Akasyah, Ranjbar & Abd-Shukor 2021). The rise in $T_{c-onset}$ with increasing sintering temperature suggests that the sample sintered at 980 °C achieved a more homogeneous YBCO-123 phase, with fewer impurities and defects, as confirmed by the XRD data in Table 2. The $T_{c-onset}$ values for YBCO-123 sintered at 920 °C, 950 °C, and 980 °C were 92.59 K, 92.24 K, and 93.21 K, respectively. The negligible rise in $T_{c-onset}$ observed between samples sintered at 920 °C and 980 °C suggests that phase formation may largely stabilize around 920 °C, with only marginal enhancements occurring at 980 °C. The lower $T_{c-onset}$ for the 950 °C sample, as measured by ACS, compared to 920 °C, likely results from rapid

oxygen diffusion during sintering, causing inhomogeneous oxygen distribution or the formation of oxygen-deficient regions. Earlier research has indicated that variations in oxygen levels during the sintering process influence $T_{c-onset}$, with elevated sintering temperatures facilitating improved oxygenation, which is essential for obtaining higher T_c values in YBCO (Hannachi et al. 2022; Kulpa et al. 1989). Comparing these ACS results to those from the four-point probe (4PP) measurements, both techniques show an increase in $T_{c-onset}$ with higher sintering temperature as shown in Figure 5. Sintering at elevated temperatures generally improves phase purity and reduces defects, enhancing T_c values in YBCO. While the 4PP method is sensitive to local inhomogeneities and surface imperfections, ACS provides a more comprehensive analysis of the bulk superconducting properties, particularly in samples with uniform oxygen content and minimal surface defects (Bartůnek et al. 2019; Koblischka-Veneva et al. 2019; Nur-Akasyah, Ranjbar & Abd-Shukor 2021; Ryad Alhadei et al. 2024a).

In the imaginary part of the AC susceptibility (χ''), representing the out-of-phase component, the intergranular losses are observed. The loss peaks, caused by energy dissipation due to flux motion between grains,

are sharper and narrower in samples sintered at 980 °C compared to those sintered at lower temperatures. The shift of the loss peaks to lower temperatures and their broadening at lower sintering temperatures indicate a reduction in flux pinning strength. A larger peak shift suggests weaker flux pinning (Aima et al. 2016; Kameli, Salamati & Abdolhosseini 2008). The coupling peak temperature (T_p), which signifies the maximum hysteresis loss due to vortex motion, ranges between 91.49 K and 92.48 K for all samples. At this temperature, flux begins to penetrate the samples, and vortex motion is pinned by diamagnetic shielding. Full flux penetration is reached at (T_p) (Nurhidayah et al. 2018). Among the samples, the intergranular loss peak is most pronounced in the sample sintered at 950 °C, with (T_p) 91.49 K. As the sintering temperature increased, (T_p) shifted to higher temperatures and became narrower, indicating enhanced flux pinning and intergranular coupling (Poonam, Jha & Awana 2013). Table 4 summarizes the onset temperature of diamagnetism ($T_{c-onset}$), coupling peak temperature (T_p), the ratio of ($T_p/T_{c-onset}$), and the intergranular current density J_{cm} at T_p . The ratio of ($T_p/T_{c-onset}$) is used to describe the coupling strength between grains, where a higher ratio signifies stronger coupling between superconducting grains (Deac et al. 1999). The intergranular current density J_{cm} was calculated using the Bean model equation (Bean 1962; Kameli, Salamati & Abdolhosseini 2008):

$$J_{cm}(T_p) = \frac{H}{\sqrt{(ab)}} \quad (1)$$

where H is the applied AC magnetic field; a and b represent the dimensions of the rectangular bar-shaped cross section of the sample ($2a \times 2b$). The values of $J_{cm}(T_p)$ values for all samples ranged from approximately 7.629 to 7.639 A/cm². Figure 6 shows the variation in T_p and J_{cm} for YBCO samples sintered at different temperatures. The sample sintered at 980 °C demonstrated the highest $T_{c-onset}$, T_p and J_{cm} values. This enhancement is attributed to the optimized crystal structure, robust intergranular connectivity, and efficient flux pinning achieved at higher sintering temperatures. The improved J_{cm} , a critical parameter for Y-123 applications, directly relates to the material's maximum current-carrying capacity. This result has a good agreement with the XRD and 4PP analysis. To summarize, AC susceptibility (ACS) is a preferred technique for investigating the superconducting properties of granular YBCO bulk ceramic. This non-destructive method eliminates the need for electrical contacts, making it suitable for small or powdered samples. In polycrystalline Y-123, ACS measurements often show a two-step diamagnetic transition, indicative of both intra-granular and inter-granular superconducting behavior.

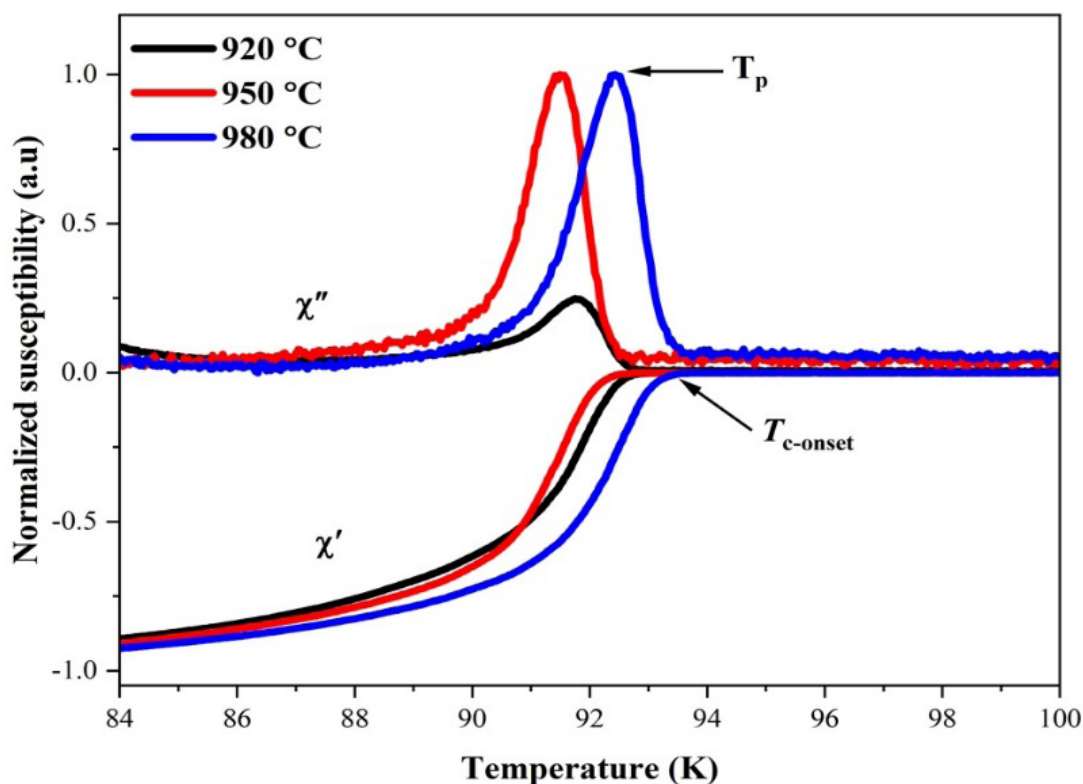


FIGURE 4. Presents the temperature-dependent AC susceptibility curves for YBCO samples sintered at different temperatures

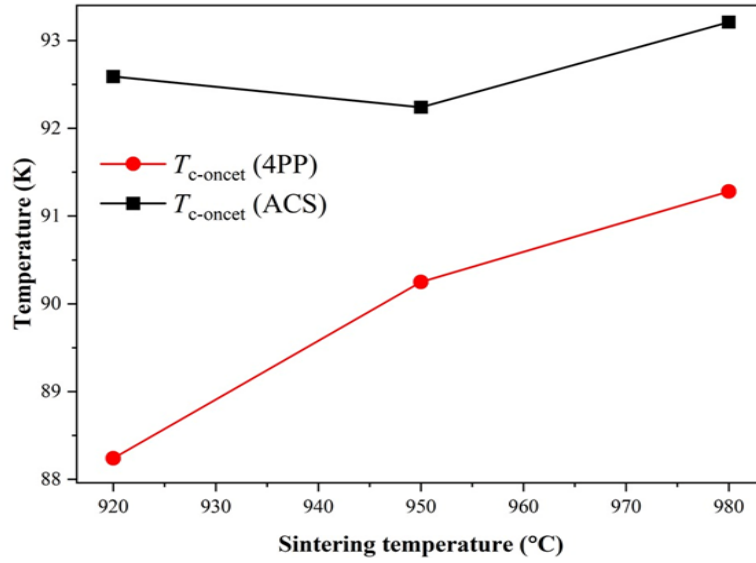


FIGURE 5. Shows the correlation between the critical temperature ($T_{c-onset}$) as measured by (4PP) and (ACS) techniques for YBCO samples sintered at different temperatures

TABLE 4. Summarizes the data for the onset temperature of diamagnetism ($T_{c-onset}$), coupling peak temperature (T_p), the ratio of ($T_p/T_{c-onset}$), and the intergranular current density J_{cm} at T_p

Sintering temperatures (°C)	$T_{c-onset}$ (K)	T_p (K)	$T_p/T_{c-onset}$ (K)	J_{cm} A/cm ²
920	92.59	91.75	0.991	7.629
950	92.24	91.49	0.992	7.632
980	93.21	92.48	0.993	7.639

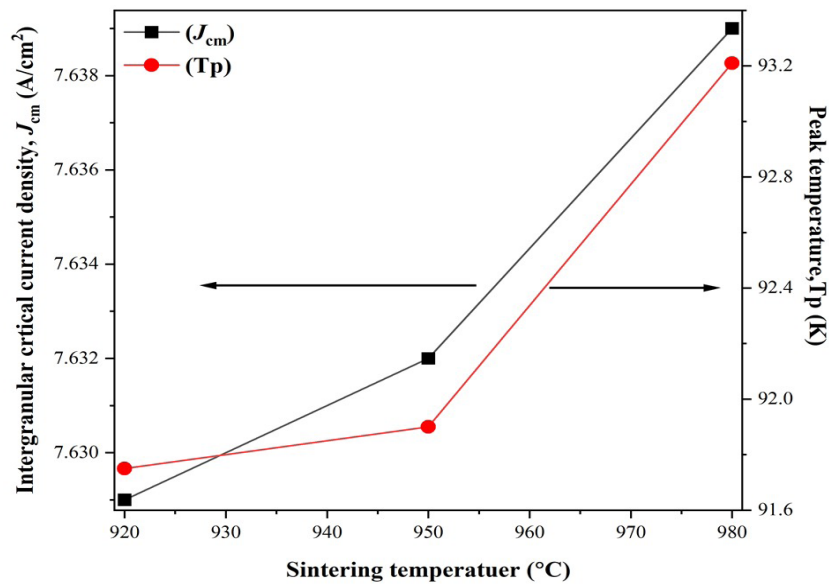


FIGURE 6. Variation of peak temperature (T_p) and intergranular critical current density (J_{cm}) for YBCO samples sintered at different temperatures. Solid lines are provided as visual guides only

CONCLUSION

YBa₂Cu₃O_{7-δ} (YBCO) bulk ceramics were successfully synthesized using the solid-state reaction method and subjected to three different sintering temperatures. The sample sintered at 980 °C achieved the highest phase purity (98.9%), larger crystallite size, narrowest resistive transition width (ΔT_c), and the best superconducting transition temperature ($T_{c-onset}$). Both electrical resistivity and AC susceptibility measurements confirmed that sintering at higher temperatures leads to better grain connectivity, phase purity, coupling peak temperature (T_p), and enhanced flux pinning, resulting in superior superconducting properties. These findings recommend that the sintering at elevated temperatures approaching the melting point of YBCO (980 °C) is crucial for achieving the best performance in YBCO bulk ceramics. Subsequent studies could investigate the impact of more precise temperature adjustments and various doping strategies to further enhance the superconducting properties of YBCO for practical applications.

ACKNOWLEDGEMENTS

This research was supported by the Ministry of Higher Education (MOHE), Malaysia under FRGS Grant No. FRGS/1/2024/STG05/UPM/02/4 and this paper was partly supported by Japan Science and Technology Agency (JST) for advanced Project Based Learning (aPBL), Shibaura Institute of Technology (SIT) under Top Global University Project, designed by the Ministry of Education, Culture, Sports, and Science & Technology in Japan.

REFERENCES

- Abdul Hussein, A.A., Abdul Hussein, A.M. & Hasan, N.A. 2023. Study of the properties of YBCO superconductor compound in various preparation methods: A short review. *Journal of Applied Sciences and Nanotechnology* 3(1): 65-79. <https://www.iasj.net/iasj/download/fb012650d9a005d5>
- Aima Ramli, Abdul Halim Shaari, Chen Soo Kean & Mohd Mustafa Awang Kechik. 2018. The effect of Sm₂O₃ nanoparticle inclusion on superconducting properties of YBCO ceramics. *ASM Sci. J. Special Issue* 2018(1): 9-16. [https://doi.org/10.1016/S1002-0721\(16\)60112-6](https://doi.org/10.1016/S1002-0721(16)60112-6)
- Aima Ramli, Abdul Halim Shaari, Hussein Baqiah, Chen Soo Kean, Mohd Mustafa Awang Kechik & Zainal Abidin Talib. 2016. Role of Nd₂O₃ nanoparticles addition on microstructural and superconducting properties of YBa₂Cu₃O_{7-δ} ceramics. *Journal of Rare Earths* 34(9): 895-900.
- Aşıkuzun, E. & Öztürk, Ö. 2020. Theoretical and experimental comparison of micro-hardness and bulk modulus of orthorhombic YBa₂Cu_{3-x}Zn_xO superconductor nanoparticles manufactured using sol-gel method. *Sakarya University Journal of Science* 24(5): 854-864. <https://doi.org/10.16984/soaufenbilder.676028>
- Bahboh, A., Shaari, A.H., Baqiah, H., Chen, S.K., Awang Kechik, M.M., Talib, Z.A. & Dihom, M.M. 2019. Effect of sol-gel synthesized BiFeO₃ nanoparticle addition in YBa₂Cu₃O_{7-δ} (Y123) superconductor synthesized by standard solid state reaction method. *Solid State Phenomena* 290: 245-251. <https://www.scientific.net/SSP.290.245>
- Barood, F., Awang Kechik, M.M., Tee, T.S., Kien, C.S., Pah, L.K., Hong, K.J., Shaari, A.H., Baqiah, H., Abdul Karim, M.K. & Shabdin, M.K. 2023. Orthorhombic YBa₂Cu₃O_{7-δ} superconductor with TiO₂ nanoparticle addition: Crystal structure, electric resistivity, and AC susceptibility. *Coatings* 13(6): 1093. <https://doi.org/10.3390/coatings13061093>
- Bartůněk, V., Luxa, J., Sedmidubský, D., Hlásek, T. & Jankovský, O. 2019. Microscale and nanoscale pinning centres in single-domain REBCO superconductors. *Journal of Materials Chemistry C* 7(42): 13010-13019. <https://pubs.rsc.org/en/content/articlehtml/2019/tc/c9tc01455a>
- Bean, C.P. 1962. Magnetization of hard superconductors. *Physical Review Letters* 8(6): 250.
- Benzi, P., Bottizzo, E. & Rizzi, N. 2004. Oxygen determination from cell dimensions in YBCO superconductors. *Journal of Crystal Growth* 269(2-4): 625-629. <https://doi.org/10.1016/j.jcrysgro.2004.05.082>
- Campi, G., Ricci, A., Poccia, N. & Bianconi, A. 2014. Imaging spatial ordering of the oxygen chains in YBa₂Cu₃O_{6+y} at the insulator-to-metal transition. *Journal of Superconductivity and Novel Magnetism* 27: 987-990. <https://doi.org/10.1007/s10948-013-2434-7>
- Chen, X., Yang, S., Chen, Y., Wang, L., Zhang, Y., Feng, Y. & Zhao, Y. 2022. Phase formation and superconductivity of Nb₃Al bulk materials prepared by spark plasma sintering and powder metallurgy. *Journal of Superconductivity and Novel Magnetism* 35(9): 2339-2347. <https://doi.org/10.1007/s10948-022-06271-z>
- Cheong, C.M. & Chen, S.K. 2024. Characterization of YBa₂Cu₄O₈ superconductor prepared by using YBa₂Cu₃O_{7-x} and CuO via solid state reaction technique with heating under ordinary oxygen pressure. *Materials Today: Proceedings* 96: 50-54. <https://doi.org/10.1016/j.matpr.2023.09.212>
- Chin, T.S., Huang, T.W., Lin, W.T., Wu, N.C., Chou, Y.H., Wu, T.C., Wu, P.T. & Yen, H.H. 1987. The formation of Y-Ba-Cu-O phases during solid state reaction. *MRS Online Proceedings Library* 99: 261-264. <https://doi.org/10.1557/PROC-99-261>
- Deac, I.G., Burzo, E., Pop, A.V., Pop, V., Tetean, R., Kovacs, D. & Borodi, G. 1999. Intergranular properties of (Y_{1-xy}Zr_xCa_y)Ba₂Cu₃O_{7-δ} compounds. *International Journal of Modern Physics B* 13(13): 1645-1654. <https://doi.org/10.1142/S0217979299001624>

- Dubinsky, S., Lumelsky, Y., Grader, G.S., Shter, G.E. & Silverstein, M.S. 2005. Thermal degradation of poly(acrylic acid) containing metal nitrates and the formation of $\text{YBa}_2\text{Cu}_3\text{O}_{7-x}$. *Journal of Polymer Science Part B: Polymer Physics* 43(10): 1168-1176.
- Farneth, W.E., Bordia, R.K., McCarron III, E.M., Crawford, M.K. & Flippen, R.B. 1988. Influence of oxygen stoichiometry on the structure and superconducting transition temperature of $\text{YBa}_2\text{Cu}_3\text{O}_x$. *Solid State Communications* 66(9): 953-959. [https://doi.org/10.1016/0038-1098\(88\)90545-5](https://doi.org/10.1016/0038-1098(88)90545-5)
- Hannachi, E., Mahmoud, K.A., Sayyed, M.I. & Slimani, Y. 2022. Effect of sintering conditions on the radiation shielding characteristics of YBCO superconducting ceramics. *Journal of Physics and Chemistry of Solids* 164: 110627
- Hong, S., Kim, R.S., Qi, Y., Zhao, X., Kim, S.H. & Ryu, Y.G. 2023. Thermal decomposition of precursor of $\text{YBa}_2\text{Cu}_3\text{O}_{7-\delta}$ superconducting layer. *Reaction Kinetics, Mechanisms and Catalysis* 136(5): 2801-2813. doi: <https://doi.org/10.1007/s11144-023-02486-w>
- Howe, B.A. 2014. *Crystal Structure and Superconductivity of $\text{YBa}_2\text{Cu}_3\text{O}_{7-x}$* . Mankato: Minnesota State University.
- Jin, F., Zhang, H., Wang, W., Liu, X. & Chen, Q. 2017. Improvement in structure and superconductivity of $\text{YBa}_2\text{Cu}_3\text{O}_{6+y+\delta}$ ceramics superconductors by optimizing sintering processing. *Journal of Rare Earths* 35(1): 85-89. [https://doi.org/10.1016/S1002-0721\(16\)60177-1](https://doi.org/10.1016/S1002-0721(16)60177-1)
- Kamarudin, A.N., Awang Kechik, M.M., Abdullah, S.N., Baqiah, H., Chen, S.K., Abdul Karim, M.K., Ramli, A., Lim, K.P., Shaari, A.H. & Miryala, M. 2022. Effect of graphene nanoparticles addition on superconductivity of $\text{YBa}_2\text{Cu}_3\text{O}_{7-\delta}$ synthesized via the thermal treatment method. *Coatings* 12(1): 91. <https://www.mdpi.com/2079-6412/12/1/91>
- Kameli, P., Salamati, H. & Abdolhosseini, I. 2008. AC susceptibility study of $\text{Bi}_{1-x}\text{Pb}_x\text{Sr}_2\text{Ca}_{2-x}\text{Mg}_x\text{Cu}_3\text{O}_y$ ($x= 0, 0.2$ and 0.4) superconductor systems. *Journal of Alloys and Compounds* 458 (1-2): 61-65.
- Koblischka-Veneva, A., Koblischka, M.R., Berger, K., Nouailhetas, Q., Douine, B., Muralidhar, M. & Murakami, M. 2019. Comparison of temperature and field dependencies of the critical current densities of bulk YBCO, MgB_2 , and iron-based superconductors. *IEEE Transactions on Applied Superconductivity* 29(5): 1-5 <https://ieeexplore.ieee.org/abstract/document/8649756>
- Kulpa, A., Chaklader, A.C.D., Osborne, N.R., Roemer, G., Sullivan, B. & Williams, D.LI. 1989. Influence of oxygen ordering and sintering temperatures on the superconducting transition temperature of $\text{YBa}_2\text{Cu}_3\text{O}_x$ compound at fixed oxygen content x higher than $x= 6.8$. *Solid State Communications* 71(4): 265-268. [https://doi.org/10.1016/0038-1098\(89\)91011-9](https://doi.org/10.1016/0038-1098(89)91011-9)
- Mohammad Rasti & Mohammad Reza Mohammadzadeh. 2020. Fabrication of YBCO thin films by fluorine-free MOCSD method: Influence of sintering near the melting point. *IEEE Transactions on Applied Superconductivity* 30(6): 1-8. <https://ieeexplore.ieee.org/abstract/document/9050541>
- Mustafa Mousa Dihom, Abdul Halim Shaari, Hussein Baqiah, Naif Mohammed Al-Hada, Chen, Soo Kean, Rabaah Syahidah Azis, Mohd Mustafa Awang Kechik & R. Abd-Shukor. 2017. Effects of calcination temperature on microstructure and superconducting properties of Y123 ceramic prepared using thermal treatment method. *Solid State Phenomena* 268: 325-329. <https://www.scientific.net/SSP.268.325>
- Nazarudin, M.F., Hamadneh, I., Tan, W.T. & Zainal, Z. 2011. The effect of sintering temperature variation on the superconducting properties of $\text{ErBa}_2\text{Cu}_3\text{O}_{7-\delta}$ superconductor prepared via coprecipitation method. *Journal of Superconductivity and Novel Magnetism* 24: 1745-1750.
- Nur-Akasyah, J., Abd-Shukor, R. & Chong, T.V. 2023. Elemental substitution at Tl site of $\text{Tl}_{1-x}\text{X}_x$ (Ba, Sr) CaCu_2O_7 superconductor with $X= \text{Cr, Bi, Pb, Se, and Te}$. *Materials* 16(11): 4022. <https://doi.org/10.1016/j.ceramint.2021.08.078>
- Nur-Akasyah, J., Ranjbar, M.G. & Abd-Shukor, R. 2021. Influence of Se and Te substitutions at Tl-site of Tl (Ba, Sr) CaCu_2O_7 superconductor on the AC susceptibility and electrical properties. *Ceramics International* 47(22): 31920-31926.
- Nurhidayah Mohd Hapipi, Soo Kien Chen, Abdul Halim Shaari, Mohd Mustafa Awang Kechik, Kar Ban Tan & Kean Pah Lim. 2018. Superconductivity of Y_2O_3 and BaZrO_3 nanoparticles co-added $\text{YBa}_2\text{Cu}_3\text{O}_{7-\delta}$ bulks prepared using co-precipitation method. *Journal of Materials Science: Materials in Electronics* 29(21): 18684-18692. doi: 10.1007/s10854-018-9991-2
- Nurhidayah Mohd Hapipi, Abdul Halim Shaari, Mohd Mustafa Awang Kechik, Kar Ban Tan, Roslan Abd-Shukor, Nurul Raihan Mohd Suib & Soo Kien Chen. 2017. Effect of heat treatment condition on the phase formation of $\text{YBa}_2\text{Cu}_3\text{O}_{7-\delta}$ superconductor. *Solid State Phenomena* 268: 305-310. <https://www.scientific.net/ssp.268.305>
- Nur Afiqah Mohamed Indera Alim Sah, Mohd Mustafa Awang Kechik, Chen Soo Kien, Lim Kean Pah, Abdul Halim Shaari, Muhammad Kashfi Shabdin, Muhammad Khalis Abdul Karim, Muralidhar Miryala, Hussein Baqiah, Khairul Khaizi Mohd Shariff, Yap Siew Hong & Arebat Ryad Alhadei Mohamed. 2024. Comparative studies of pure $\text{YBa}_2\text{Cu}_3\text{O}_{7-\delta}$ prepared by modified thermal decomposition method against thermal treatment method. *Applied Physics A* 130(5): 340. doi: 10.1007/s00339-024-07412-y

- Nur Athirah Che Dzul-Kifli, Mohd Mustafa Awang Kechik, Hussein Baqiah, Abdul Halim Shaari, Kean Pah Lim, Soo Kien Chen, Safia Izzati Abd Sukor, Muhammad Kashfi Shabdin, Muhammad Khalis Abdul Karim, Khairul Khaizi Mohd Shariff & Muralidhar Miryala. 2022. Superconducting properties of $\text{YBa}_2\text{Cu}_3\text{O}_{7-\delta}$ with a multiferroic addition synthesized by a capping agent-aided thermal treatment method. *Nanomaterials* 12(22): 3958. <https://doi.org/10.3390/nano12223958>
- Nur Nabilah Mohd Yusuf, Mohd Mustafa Awang Kechik, Hussein Baqiah, Chen Soo Kien, Lim Kean Pah, Abdul Halim Shaari, Wan Nur Wathiq Wan Jusoh, Safia Izzati Abd Sukor, Mustafa Mousa Dihom & Zainal Abidin Talib. 2018. Structural and superconducting properties of thermal treatment-synthesised bulk $\text{YBa}_2\text{Cu}_3\text{O}_{7-\delta}$ superconductor: Effect of addition of SnO_2 nanoparticles. *Materials* 12(1): 92. <https://doi.org/10.3390/ma12010092>
- Ozturk, O., Arebat, R.A.M., Nefrow, A.R.A., Bulut, F., Guducu, G., Asikuzun, E. & Celik, S. 2019. Investigation of structural, superconducting and mechanical properties of Co/Cu substituted YBCO-358 ceramic composites. *Journal of Materials Science: Materials in Electronics* 30(8): 7400-7409. doi: 10.1007/s10854-019-01053-1
- Pathak, L.C., Mishra, S.K., Das, S.K., Bhattacharya, D. & Chopra, K.L. 2001. Effect of sintering atmosphere on the weak-link behaviour of YBCO superconductors. *Physica C: Superconductivity* 351(3): 295-300. [https://doi.org/10.1016/S0921-4534\(00\)01628-2](https://doi.org/10.1016/S0921-4534(00)01628-2)
- Poonam, R., Jha, R. & Awana, V.P.S. 2013. AC susceptibility study of superconducting $\text{YBa}_2\text{Cu}_3\text{O}_7$: Ag_x bulk composites ($x= 0.0-0.20$): The role of intra and intergranular coupling. *Journal of Superconductivity and Novel Magnetism* 26: 2347-2352. <https://doi.org/10.1007/s10948-013-2203-7>
- Pruss, N., Kraak, W., Müller, H-U., Jacobi, A., Dwelk, H. & Herrmann, R. 1989. Influence of the sintering temperature on the physical properties of $\text{YBa}_2\text{Cu}_3\text{O}_{7-\delta}$ ceramic samples. *Physica Status Solidi (a)* 116(2): 793-801. <https://doi.org/10.1002/pssa.2211160240>
- Reissner, M., Steiner, W., Stroh, R., Hörhager, S., Schmid, W. & Wruss, W. 1990. Influence of sintering temperature on the superconducting properties of $\text{YBa}_2\text{Cu}_3\text{O}_{7-x}$. *Physica C: Superconductivity* 167(5-6): 495-502. [https://doi.org/10.1016/0921-4534\(90\)90665-2](https://doi.org/10.1016/0921-4534(90)90665-2)
- Ryad Alhadei Mohamed Arebat, Mohd Mustafa Awang Kechik, Chen Soo Kien, Lim Kean Pah, Hussien Baqiah, Khairul Khaizi Mohd Shariff, Abdul Halim Shaari, Muralidhar Miryala, Yap Siew Hong & Nur Afiqah Indera Mohamed Indera Alim Sah. 2024a. $\text{YBa}_2\text{Cu}_3\text{O}_{7-d}$ bulk superconductors: Exploring the impact of two synthesis techniques on the microstructure and critical temperature. *Solid State Science and Technology* 32(2): 28-41. <https://myjms.mohe.gov.my/index.php/masshp/article/view/25985>
- Ryad Alhadei Mohamed Arebat, Mohd Mustafa Awang Kechik, Chen Soo Kien, Lim Kean Pah, Hussien Baqiah, Khairul Khaizi Mohd Shariff, Yap Siew Hong, Hoo Keong Peh, Abdul Halim Shaari, Syahrul Humaidi & Muralidhar Miryala. 2024b. Enhancing superconducting properties of $\text{YBa}_2\text{Cu}_3\text{O}_{7-\delta}$ through Nd_2O_3 addition prepared using modified thermal decomposition method. *Applied Physics A* 130(12): 897. doi: 10.1007/s00339-024-08035-z
- Yap Siew Hong, Mohd Mustafa Awang Kechik, Hussien Baqiah, Soo Kien Chen, Kean Pah Lim, Muhammad Kashfi Shabdin, Mohd Hafiz Mohd Zaid, Yazid Yaakob, Mohd Khalis Abdul Karim, Zhi Wei Loh, Abdul Halim Shaari & Muralidhar Miryala. 2024a. Comparative study of superconducting properties for $\text{YBa}_2\text{Cu}_3\text{O}_{7-\delta}$ added Ca-compounds synthesized under different annealing conditions. *Solid State Science and Technology* 31(2): 71-81.
- Yap Siew Hong, Mohd Mustafa Awang Kechik, Fitri Khoerunnisa, Hussien Baqiah, Soo Kien Chen, Kean Pah Lim, Muhammad Kashfi Shabdin, Mohd Hafiz Mohd Zaid, Yazid Yaakob, Mohd Khalis Abdul Karim, Syahrul Humaidi, Abdul Halim Shaari & Muralidhar Miryala. 2024b. Microstructural and excess conductivity properties of Y-123: Effect of organic polymer chitosan inclusion. *Journal of Materials Science: Materials in Electronics* 35(21): 1452.
- Yap Siew Hong, Mohd Mustafa Awang Kechik, Khairul Khaizi Mohd Shariff, Hussien Baqiah, Soo Kien Chen, Kean Pah Lim, Muhammad Kashfi Shabdin, Mohd Hafiz Mohd Zaid, Yazid Yaakob, Mohd Khalis Abdul Karim, Syahrul Humaidi, Abdul Halim Shaari & Muralidhar Miryala. 2024c. Fluctuation induces conductivity and microstructural studies in Y-123: Effect of CaO inclusion. *Journal of Alloys and Compounds* 1005: 175955. <https://doi.org/10.1016/j.jallcom.2024.175955>
- Yeoh, L.M. & Abd-Shukur, R. 2008. The study on various wet chemistry techniques on $\text{YBa}_2\text{Cu}_3\text{O}_{7-\delta}$ superconducting oxides powder preparation. *Journal of Non-Crystalline Solids* 354(34): 4043-4048. <https://www.sciencedirect.com/science/article/pii/S0022309308003190>
- Zhou, M., Sun, A., Sun, L. & Han, P. 2013. Effect of the oxygen distribution and inhomogeneity on the superconducting properties of $\text{YBa}_2\text{Cu}_3\text{O}_{7-\delta+x}$ mol% $\text{Y}_2\text{Ba}_4\text{CuMoO}_y$ superconductors. *Superconductor Science and Technology* 26(10): 105006. <https://iopscience.iop.org/article/10.1088/0953-2048/26/10/105006/meta>

*Corresponding author; email: mmak@upm.edu.my